Neurosurgical Review (2019) 42:433–441
https://doi.org/10.1007/s10143-018-0981-x

ORIGINAL ARTICLE

Imaging scoring systems for preoperative molecular diagnoses of lower-grade gliomas

Tokunori Kanazawa[1] · Hirokazu Fujiwara[2] · Hidenori Takahashi[2] · Yuya Nishiyama[3] · Yuichi Hirose[3] · Saeko Tanaka[1] · Kazunari Yoshida[1] · Hikaru Sasaki[1]

Received: 21 January 2018 / Revised: 4 April 2018 / Accepted: 17 April 2018 / Published online: 26 April 2018

Abstract

Recent advance in molecular characterization of gliomas showed that patient prognosis and/or tumor chemosensitivity correlate with certain molecular signatures; however, this information is available only after tumor resection. If molecular information is available by routine radiological examinations, surgical strategy as well as overall treatment strategy could be designed preoperatively.With the aim to establish an imaging scoring system for preoperative diagnosis of molecular status in lower-grade gliomas (WHO grade 2 or 3, LrGGs), we investigated 8 imaging features available on routine CT and MRI in 45 LGGs (discovery cohort) and compared them with the status of 1p/19q codeletion, *IDH* mutations, and *MGMT* promoter methylation. The scoring systems were established based on the imaging features significantly associated with each molecular signature, and were tested in the another 52 LrGGs (validation cohort).For prediction of 1p/19q codeletion, the scoring system is composed of calcification, indistinct tumor border on T1, paramagnetic susceptibility effect on T1, and cystic component on FLAIR. For prediction of *MGMT* promoter methylation, the scoring system is composed of indistinct tumor border, surface localization (FLAIR), and cystic component. The scoring system for prediction of *IDH* status was not established. The 1p/19q score ≥ 3 showed PPV of 96.2% and specificity of 98.1%, and the *MGMT* methylation score ≥ 2 showed PPV of 77.4% and specificity of 67.6% in the entire cohort.These scoring systems based on widely available imaging information may help to preoperatively design personalized treatment in patients with LrGG.

Keywords Glioma · Imaging · MRI · Personalized treatment · Preoperative molecular diagnosis

Introduction

Although there has been an enormous progress in molecular characterization of gliomas, the initial maximal safe resection is still the gold standard of surgery for diffuse gliomas based on the evidence that more extensive surgical resection is associated with longer life expectancy for both low-grade and high-grade gliomas [25, 28]. Indeed, molecular information relevant to treatment strategy is informed only after surgical resection. However, if the molecular signature of the tumor is informed before initial surgery, such information could influence the overall treatment strategy as well as initial surgical strategy; the tumor with molecular signature suggesting indolent tumor growth or chemosensitivity could be subjected to resection weighting the safety rather than radicality, and the tumor with information suggesting aggressive behavior or insensitivity to chemotherapy should perhaps be resected as much as safely possible with the possible risk of functional sequela. The initial biopsy may occasionally be indicated; however, craniotomy is required even for biopsy in most cases.

There have been many studies on the association between imaging features and specific genetic alterations in gliomas,

Electronic supplementary material The online version of this article (https://doi.org/10.1007/s10143-018-0981-x) contains supplementary material, which is available to authorized users.

✉ Hikaru Sasaki
hsasaki@keio.jp

[1] Department of Neurosurgery, Keio University School of Medicine, 35 Shinanomachi, Shinjuku-ku, Tokyo 160-8582, Japan

[2] Department of Diagnostic Radiology, Keio University School of Medicine, 35 Shinanomachi, Shinjuku-ku, Tokyo 160-8582, Japan

[3] Department of Neurosurgery, Fujita Health University School of Medicine, 1-98 Dengakugakubo, Kutusukake-cho, Toyoake, Aichi 470-1192, Japan

with clinically relevant results [1, 3, 5, 11, 18, 24, 29, 31, 35, 36]. For example, Zlatescu et al. demonstrated an association between genetic signature and tumor location for the first time [36], and Megyesi et al. reported that oligodendrogliomas with 1p and 19q loss were more likely to have an indistinct tumor border on T1-weighted MRI, possibly indicative of invasiveness [18]. However, these findings are not utilized in daily practice for therapeutic decision-making due to inter-observer bias, insufficient specificity, or novel technique that is not commonly available. Recently, we have demonstrated that the combination of two simple imaging features, tumor calcification and surface localization (SL) predicts the presence of 1p/19q codeletion with high positive predictive value (PPV) and specificity [21]. To avoid ineffective chemotherapy, prediction with low false-positive rate, i.e., high specificity/PPV rather than high sensitivity, is favored; however, the sensitivity of the combination of calcification and SL was not sufficient, leaving more than half of the codeleted tumors out of the preoperative prediction. In the present paper, we aimed to establish the scoring system composed of several imaging characterisitics provided by routine CT and MRI to preoperatively predict important molecular signature with sufficient sensitivity as well as high specificity/PPV. Presence or absence of 1p/19q codeletion, promoter methylation of the *O6-methylguanine-DNA methyltransferase (MGMT)* gene, and mutations in *isocitrate dehydrogenase (IDH)* genes were compared with the imaging features suggested to correlate with those molecular signatures in the literature, and the scoring system was tested in the two independent cohorts.

Materials and methods

Clinical samples

Pathology records of brain tumors treated at the Department of Neurosurgery, Keio University Hospital in 2006 or later were reviewed, and the eligibility criteria included the following: (a) newly diagnosed, untreated diffuse glioma of WHO grade II or III; (b) preoperative CT and MRI (T1, T1 post-contrast, fluid-attenuated inversion recovery (FLAIR)) images. As a result, 45 tumors that fulfilled those criteria constituted the discovery cohort. Similarly, the validation cohort was composed of 52 newly diagnosed, diffuse gliomas of WHO grade II or III resected at Fujita Health University Hospital between 2007 and 2015. The histopathological diagnosis was based on local diagnosis at each institute according to WHO criteria [13, 14, 16, 17, 37]. This study has been conducted as a part of the collaborative translational research approved by the Institutional Review Board at Keio University and Fujita Health University. Written informed consent was obtained from all patients included in the study.

Scoring of radiological characteristics

CT (plain) images and T1-weighted, T1-weighted with gadolinium (Gd) administration, and FLAIR MRI images were used for the scoring of imaging features, and all of the available sections of these images were taken into consideration for the evaluation. Parameters of T1-weighted image of discovery cohort in Keio University Hospital were repetition time (TR): < 560 ms, echo time (TE): < 9 ms and flip angle: 90° at 1.5T and TR: < 600 ms, TE: < 12 ms and flip angle: 90° at 3T, and those of the validation cohort in Fujita Health University Hospital were TR: < 645 ms, TE: < 13 ms and flip angle: 90° at 1.5T. The following imaging characteristics were selected and evaluated based on the literature review [1, 3, 11, 18, 24, 29, 31, 36]: (a) calcification on CT, present versus absent; (b) tumor border on T1-weighted images, distinct versus indistinct; (c) paramagnetic susceptibility effect on T1 (shortening on T1), present versus absent (present: presence of higher signal intensity in tumor as compared with the contralateral gray and white matter); (d) surface localization (SL) defined by more than 50% of abnormal high intensity area on FLAIR images being located within cortex, yes versus no; (e) gray matter involvement defined by abnormal high intensity involving the entire thickness of the cortex on FLAIR images, yes versus no; (f) inhomogeneous tumor signal intensity defined by presence of cystic component or similar findings on FLAIR images, present versus absent, (g) contrast enhancement on T1-weighted images with Gd administration, ring enhancement on the majority of tumor signal versus other contrast enhancement versus none; (h) temporal location defined by main location of tumor being the temporal lobe on FLAIR images, yes versus no (Fig. 1).

For the discovery cohort, imaging characteristics were assessed independently by four of the authors including two neurosurgeons (TK, HS) and two neuroradiologists (HF, HT) blinded to molecular characteristics in the tumors. The final judgment was made by consensus of three or four evaluators for each imaging characteristics. After establishment of the imaging scoring system for preoperative molecular diagnosis using the discovery cohort, the system was applied for the validation cohort. For the validation cohort, imaging characteristics were assessed independently by three neurosurgeons (TK, HS, YN) blinded to molecular characteristics in the tumors. The final judgment was made by consensus of two or three evaluators for each of the imaging characteristics included in the scoring system.

Molecular genetic analyses

Tumor DNA was extracted from microdissected pieces of formalin-fixed paraffin-embedded (FFPE) tissue as previously described [20, 27].

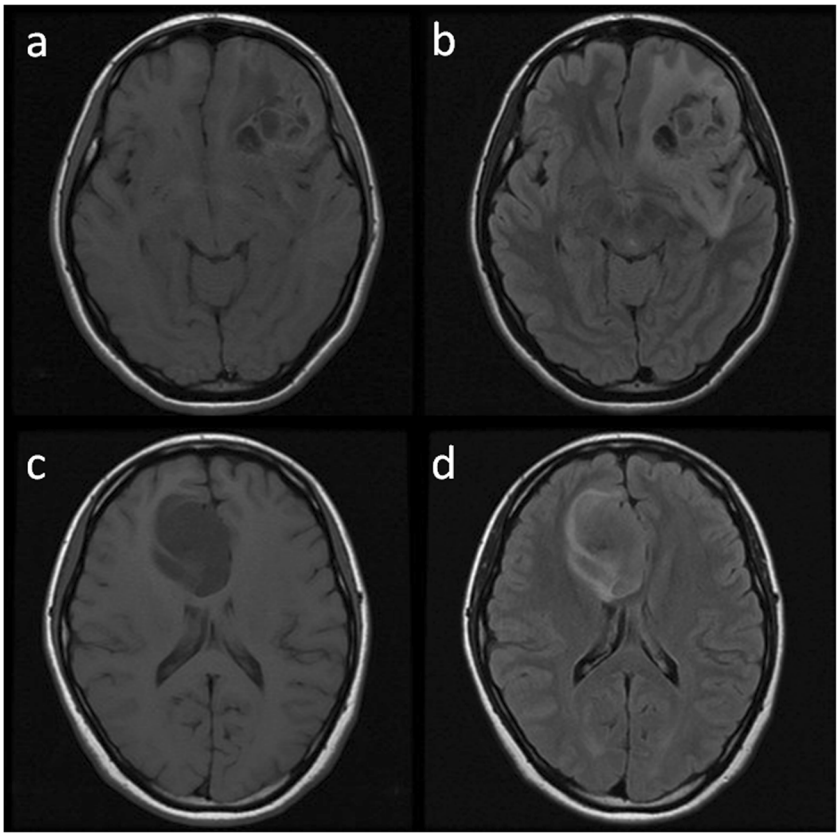

Fig. 1 Assessment of radiological features. **a**, **b** T1-weighted (**a**) and fluid-attenuated inversion recovery (FLAIR; **b**) MRI images of a 27-year-old woman with left frontal tumor. This tumor was judged as the followings: indistinct tumor border: yes, paramagnetic susceptibility effect (shortening on T1): yes, surface localization (SL): no, gray matter involvement (GMI): yes, cystic component: yes, calcification: no (not shown). 1p/19q score of this case is 3, and *MGMT* score is 2. Histologial classification of the tumor was oligoastrocytoma, and pathological diagnosis was oligodendroglioma, *IDH*-mutant and 1p/19q-codeleted. Promoter region of the *MGMT* gene was unmethylated. **c**, **d**.T1-weighted and FLAIR MRI images of a 32-year-old woman with right frontal tumor. This tumor was judged as the followings: indistinct tumor border: no, paramagnetic susceptibility effect: no, SL: yes, GMI: yes, cystic component: no, calcification: no (not shown). 1p/19q score of this case is 0, and *MGMT* score is 1. Histological classification of the tumor was oligoastrocytoma, and pathological diagnosis was diffuse astrocytoma, *IDH*-mutant (1p/19q-non-codeleted). Promoter region of the *MGMT* gene was unmethylated

1p/19q status was assessed by metaphase comparative genomic hybridization (CGH), as described previously [10, 19]. Briefly, crude tumor DNA from FFPE tissues was amplified by degenerate oligonucleotide-primed polymerase chain reaction (DOP-PCR) and was labeled with digoxigenin (DIG)-11-dUTP (Roche, Mannheim, Germany) by another DOP-PCR. Reference DNA was amplified from a 50-ng DNA obtained from normal male or female and was labeled with biotin-dUTP (Roche, Mannheim, Germany). Probe mixture was denatured and hybridized to normal metaphase spreads (Vysis, Downers Grove, IL). Unhybridized probes were washed, and the metaphase spread was incubated with a fluorescein isothiocyanate-conjugated anti-DIG antibody (Roche, Mannheim, Germany) and rhodamine-conjugated avidin (Roche, Mannheim, Germany). The preparations were washed and were counterstained with 4,6-diamino-2-phenylindole in an antifade solution. Red, green, and blue images were acquired, and ratios of fluorescence intensities along the chromosomes were determined using the CytoVision® Analysis System (Applied Imaging, San Jose, CA).

IDH mutation status was assessed by direct sequencing with polymerase chain reaction (PCR) of codon 132 in *IDH1* gene and codon 172 in *IDH2* gene using the previously described primer pairs [33]. The PCR thermal conditions consisted of an initial denaturing step of 95 °C for 3 min, followed by 40 cycles of 95 °C for 30 s, 56 °C for 30 s, 72 °C for 40 s, and finally, an extension step of 72 °C for 10 min. The resulting products were analyzed on 3% agarose gel. After purifying the PCR products, DNA-sequencing reactions were performed using the BigDye Terminator version 3.1 Cycle Sequencing kit, and sequence data were analyzed using the 3730xl DNA Analyzer (Applied Biosystems, Foster City, CA, USA).

Methylation status of the promoter region of the *MGMT* gene was analyzed by methylation-specific PCR using the EZ DNA Methylation-Direct kit (Zymo Research Corp., Orange,

CA, USA). PCR was performed with primers specific for methylated or unmethylated DNAs (Sigma-Aldrich Japan, Inc) [7] and Taq polymerase HotStart Version (Takara Taq HotStart Version; Takara Bio, Inc., Shiga, Japan), and the annealing temperature was decreased from 65 to 58 °C with 35 cycles in total. The PCR products were separated on a 4% MetaPhor Agarose gel (Lonza, Rockland, ME, USA). Control DNAs for the methylated, unmethylated, and wild-type sequence were obtained in the Chemicon CpG WIZ MGMT Amplification kit (Temecula, CA, USA).

Statistical analysis and scoring system

The predictive values of each radiological feature including sensitivity, specificity, PPV, and negative predictive value (NPV) were calculated for each molecular signature. The significance of associations between molecular signatures and radiological features was assessed in univariate analysis using the Fisher's exact test and χ^2 test. The significance level for these statistical tests was set at 0.05. Data was analyzed with the IBM SPSS Statistics 23.0 software. Multivariate analysis was not applied considering the number of outcomes and variables. The radiological features significantly associated with each molecular signature on univariate analyses in the discovery cohort were included in the scoring system. In therapeutic decision-making, high PPV/specificity is important to avoid ineffective chemotherapy, and the threshold of the scoring system was placed based on PPV.

Results

Discovery cohort

The discovery cohort consisted of 45 diffuse gliomas of grade II or III based on the original institutional diagnoses. (Table S1) These tumors arose in 25 men and 20 women, with a mean age of 46 years old at the time of surgery (range, 23–81 years). The tumors included 32 grade II tumors (4 diffuse astrocytomas, 21 oligodendrogliomas, 7 oligoastrocytomas), and 13 grade III tumors (2 anaplastic astrocytomas, 9 anaplastic oligodendrogliomas, 2 anaplastic oligoastrocytomas). Total loss of chromosomes 1p and 19q were observed in 29 of 45 tumors, *MGMT* promoter methylation in 27 of 45 tumors, and *IDH* mutations in 40 of 45 tumors.

Table 1 shows predictive values and *p* values of each imaging characteristics for 1p/19q codeletion. Twenty-two of the 45 patients were examined with 3T MRI, and the other 23 were with 1.5T. Calcification, indistinct tumor border on T1, paramagnetic susceptibility effect on T1, presence of cystic component, and temporal location were significantly associated with presence or absence of 1p/19q codeletion. On the other hand, SL, indistinct tumor border, presence of cystic component, and temporal location were significantly associated with presence or absence of *MGMT* promoter methylation (Table 2). For *IDH* mutations, non-temporal location was the sole imaging feature that was significantly associated with *IDH* status. However, PPV (62.5%) and specificity (57.1%) were thought not to be sufficiently high to predict *IDH* mutations solely by tumor location (not shown).

Scoring system

The imaging characteristics significantly associated with each favorable molecular signature on univariate analyses were included in the scoring system. For prediction of 1p/19q codeletion, each of calcification, indistinct tumor border, paramagnetic susceptibility, and cystic component counts one point (full sore: 4). Temporal location was regarded as exclusion criteria because of the low sensitivity noted in the discovery cohort as well as the previous finding that tumors in the temporal lobe was significantly less likely to harbor 1p/19q codeletion [29, 36]. Similarly, a previous study reported that the anaplastic oligodendrogliomas of histological diagnosis with ring enhancement seldom responded to chemotherapy [2]. Therefore, ring enhancement on the majority of tumor burden, which was reminiscent of glioblastomas, was also regarded as exclusion criteria based on the result of the present study as well as the previous finding. We explored the relationship of the 1p/19q score and presence or absence of 1p/19q codeletion, and, importantly, score above 2 (score 3 or 4) predicted 1p/19q codeletion with PPV of 100%, and PPV declined if the score is 2 or less (Table 3). The 1p/19q score ≥ 3 predicted 1p19q codeletion with higher sensitivity than combination of calcification and SL (Table 4).

For prediction of *MGMT* promoter methylation, each of indistinct tumor border, SL, and cystic component counts one point (full sore: 3). Temporal location was regarded as exclusion criteria. Importantly, score ≥ 2 (score 2 or 3) predicted *MGMT* methylation with PPV of 82.6%, and PPV declined if the score is 1 or less (Tables 5 and 6).

Validation cohort

The scoring systems for 1p/19q codeletion and *MGMT* promoter methylation were applied to the validation cohort. The validation cohort consisted of 52 diffuse gliomas of grade II or III based on the original institutional diagnoses (Table S2). The tumors included 31 grade II tumors (12 diffuse astrocytomas, 4 oligodendrogliomas, 15 oligoastrocytomas), and 21 grade III tumors (13 anaplastic astrocytomas, 3 anaplastic oligodendrogliomas, 5 anaplastic oligoastrocytomas). Total loss of chromosomes 1p and 19q were observed in 15 of 52 tumors, and promoter methylation of the *MGMT* gene was observed in 31 of 52 tumors.

Table 1 Predictive values for 1p/19q codeletion by imaging features in the discovery cohort

	PPV (%)	NPV (%)	Sensitivity (%)	Specificity (%)	*P* value
Calcification	94.1 (16/17)	53.6 (15/28)	55.2 (16/29)	93.8 (15/16)	0.001
Surface localization	76.2 (16/21)	45.8 (11/24)	55.2 (16/29)	68.8 (11/16)	0.124
Gray matter involvement	62.5 (25/40)	20 (1/5)	86.2 (25/29)	6.3 (1/16)	0.408
Indistint tumor border	78.8 (26/33)	75 (9/12)	89.7 (26/29)	56.3 (9/16)	0.002
Paramagnetic susceptibility effect	88.2 (15/17)	50 (14/28)	51.7 (15/29)	87.5 (14/16)	0.009
Inhomogenous tumor contents	81.0 (17/21)	50 (12/24)	58.6 (17/29)	75 (12/16)	0.030
Contrast enhancement (total $n = 45$) Ring enhancement $n = 1$ Other enhancement $n = 22$ None $n = 22$	69.6 (16/23)	40.9 (9/22)	55.2 (16/29)	56.3 (9/16)	0.463
Ring enhancement	0 (0/1)	34.1 (15/44)	0 (0/29)	93.8 (15/16)	0.715
Temporal location	12.5 (1/8)	24.3 (9/37)	3.4 (1/29)	56.3 (9/16)	0.001

PPV positive predictive value, *NPV* negative predictive value

1p19q score ≥ 3 predicted 1p/19q codeletion with PPV of 90%, specificity of 97.2%, and sensitivity of 60% (Tables 4 and 7). *MGMT* score ≥ 2 predicted *MGMT* promoter methylation with PPV of 73.3%, specificity of 57.9%, and sensitivity of 66.6% (Tables 6 and 8).

Discussion

To date, many studies have been reported to predict the important molecular signatures that are relevant to therapeutic decision-making by simple, visual qualitative evaluation of radiological images. However, the association of single imaging feature with certain molecular signature was mostly found in univariate analyses, and qualitative evaluation of each feature is prone to be subjected to interobserver variability. Therefore, researchers recently exploit quantitative methods, often with machine-learning algorithms; Brown et al. reported that quantitative texture analysis on T2-weighted images predicted 1p/19q codeletion with more than 90% of sensitivity and specificity in 55 oligodendrogliomas [1], and Zhou et al. reported that texture model predicted *IDH* mutation and 1p/19q codeletion with good to excellent area under receiver-operating characteristic curve (AUC) [35]. Although these quantitative, computerized approaches hold substantial promise to noninvasively predict molecular characteristics of glioma, these novel techniques are not generally accessible for now, and not ready for clinical use yet. In the present study, we aimed to establish a model by combination of several imaging features easily evaluable on routine, standard MRI for the daily practice until such novel techniques become widely available.

Imaging features reported to be associated with 1p/19q codeletion include calcification (CT), frontal location,

Table 2 Predictive values for MGMT promoter methylation by imaging features in the discovery cohort

	PPV (%)	NPV (%)	Sensitivity (%)	Specificity (%)	*P* value
Calcification	76.4 (13/17)	50 (14/28)	48.1 (13/27)	77.8 (14/18)	0.079
Surface localization	76.2 (16/21)	54.2 (13/24)	59.3 (16/27)	72.2 (13/18)	0.038
Gray matter involvement	57.5 (23/40)	20 (1/5)	85.2 (23/27)	5.6 (1/18)	0.325
Indistint tumor border	69.7 (23/33)	66.7 (8/12)	85.2 (23/27)	44.4 (8/18)	0.032
Paramagnetic susceptibility effect	70.6 (12/17)	46.4 (13/28)	44.4 (12/27)	72.2 (13/18)	0.259
Inhomogenous tumor contents	81.0 (17/21)	58.3 (14/24)	63.0 (17/27)	77.8 (14/18)	0.007
Contrast enhancement (ring or other)	60.9 (14/23)	40.9 (9/22)	51.9 (14/27)	50 (9/18)	0.903
Ring enhancement	0 (0/1)	38.6 (17/44)	0 (0/27)	94.4 (17/18)	0.651
Temporal location	25 (2/8)	32.4 (12/37)	7.4 (2/27)	66.7 (12/18)	0.034

PPV positive predictive value, *NPV* negative predictive value

Table 3 The relationship of the predictive score and 1p/19q codeletion in the discovery cohort

1p/19q score	1p/19q codeleted	1p/19q non-codeleted	PPV (%)
Score 0	1	6	14.3 (1/7)
Score 1	7	6	53.8 (7/13)
Score 2	5	4	55.6 (5/9)
Score 3	7	0	100 (7/7)
Score 4	9	0	100 (9/9)

PPV positive predictive value

Table 5 The relationship of the predictive score and *MGMT* promoter methylation in the discovery cohort

MGMT score	MGMT methylated	*MGMT* unmethylated	PPV (%)
Score 0	0	6	0 (0/6)
Score 1	8	8	50 (8/16)
Score 2	11	3	78.6 (11/14)
Score 3	8	1	88.9 (8/9)

PPV positive predictive value, *MGMT* O6-methylguanine-DNA methyltransferase

indistinct tumor border on T1-weighted image (MRI), paramagnetic susceptibility effect (MRI), high relative cerebral blood volume (dynamic susceptibility contrast MRI), high uptake on ^{201}Tl-single-photon emission computed tomography (SPECT), and elevated metabolism on ^{11}C-methionine positron emission tomography (PET), etc. [11, 18, 21, 24, 31, 36]. Moreover, recent quantitative analyses suggested that 1p/19q-codeleted gliomas are distinguished from the other lower-grade gliomas by tumor texture with high sensitivity and specificity [1, 35]. In the present study, we investigated all of the imaging features that were previously suggested to be associated with 1p/19q codeletion and were available on routine CT and MRI. Finally, our scoring system consisted of four relevant features, i.e., calcification on CT, indistinct tumor border on T1, paramagnetic susceptibility effect on T1, and cystic component on FLAIR with exclusion of temporal location and ring enhancement. The score will be less affected by interobserver difference by combination of four features, and the relevance of calcification, paramagnetic susceptibility effect, and cystic component is likely to reflect the importance of tumor texture. The 1p/19q score ≥ 3 predicted 1p/19q codeletion with 56.8% of sensitivity and 98.1% of specificity in the entire cohort of the present study. Although the sensitivity may not be sufficiently high yet, about two thirds of the 1p/19q-codeleted gliomas is preoperatively predicted with very low false-positive rate. Those tumors preoperatively predicted to have 1p/19q codeletion could be subjected to resection weighting the safety rather than radicality without the possible risk of functional sequela, because the extent of resection might have less impact on patient survival with 1p/19q-codeleted gliomas [9]. Moreover, the preoperative prediction of chemosensitivity could segregate the candidates to be treated with neoadjuvant strategy [26].

Prediction of methylation status of the *MGMT* gene by imaging is more challenging. Except that ring enhancement was suggested by some previous studies to be associated with unmethylated *MGMT* promoter in glioblastomas [4, 6], none of the other MRI features was reported to be associated with *MGMT* methylation status by visual assessment with consensus [8]. Ellingson et al. reported that the methylated glioblastomas have less T2/FLAIR high intensity volume than unmethylated tumors, and that the methylated tumors are lateralized to left hemisphere and the unmethylated tumors to right; these notions might be worthy of further investigation [5]. A previous study reported that quantitative texture analysis was not sufficient to predict methylation status [4]; however, another study reported that the texture analysis with machine-learning algorithms on T2-weighted images yielded an AUC of 0.85, suggesting the utility of such approach to predict *MGMT* promoter status in glioblastomas [15]. All of these attempts were performed in the cohorts with high-grade glioma or glioblastoma, and, to our knowledge, the present study may be the first to investigate imaging features to predict *MGMT* methylation status in lower-grade gliomas. Our scoring system consists of three

Table 4 Predictive values for 1p/19q codeletion by combination of imaging features in the discovery cohort and validation cohort

	PPV (%)	NPV (%)	Sensitivity (%)	Specificity (%)
The discovery cohort				
Calcification + surface localization	100(9/9)	44.4 (16/36)	31.0 (9/29)	100 (16/16)
1p/19q score (≥ 3)	100 (16/16)	55.2 (16/29)	55.2 (16/29)	100 (16/16)
The validation cohort				
Calcification + surface localization	100 (7/7)	82.2 (37/45)	46.7 (7/15)	100 (37/37)
1p/19q score (≥ 3)	90 (9/10)	85.7 (36/42)	60 (9/15)	97.2 (36/37)
The entire cohort				
1p/19q score (≥ 3)	96.2 (25/26)	73.2 (52/71)	56.8 (25/44)	98.1 (52/53)

PPV positive predictive value, *NPV* negative predictive value

Table 6 Predictive values for *MGMT* promoter methylation by a scoring system in the discovery cohort and validation cohort

	PPV (%)	NPV (%)	Sensitivity (%)	Specificity (%)
The discovery cohort				
MGMT score (≥ 2)	82.6 (19/23)	63.6 (14/22)	70.3 (19/27)	77.8 (14/18)
The validation cohort				
MGMT score (≥ 2)	73.3 (22/30)	50 (11/22)	66.6 (22/33)	57.9 (11/19)
The entire cohort				
MGMT score (≥ 2)	77.4 (41/53)	56.8 (25/44)	68.3 (41/60)	67.6 (25/37)

PPV positive predictive value, *NPV* negative predictive value, *MGMT* O6-methylguanine-DNA methyltransferase

features, i.e., indistinct tumor border on T1, SL, and cystic component on FLAIR with exclusion of temporal location, and score ≥ 2 predicted *MGMT* promoter methylation with good PPV and moderate specificity (PPV: 77.4%, sensitivity: 68.3%, specificity: 67.6% in the entire cohort). By coupling with 1p/19q scoring system, a considerable portion of chemosensitive gliomas could be preoperatively segregated. Indeed, the interim analysis of the phase III trial in anaplastic gliomas lacking 1p/19q codeletion suggested that *MGMT* methylation is independently associated with patient survival with those tumors [30], and the preoperative prediction of *MGMT* methylation could have impact on the treatment and surgical strategy for non-codeleted LrGGs [26].

The literature suggests that *IDH*-mutant gliomas might be associated with frontal, temporal, and insular locations, lower maximal fractional anisotropy (FA)/greater minimal apparent diffusion coefficient (ADC), sharp tumor margin, and homogeneous intensity [23, 29, 32]. However, we were not successful to establish a scoring system for *IDH* mutations in the present study. Indeed, Zhou et al. reported lower AUC and sensitivity/specificity for prediction of *IDH* mutations than 1p/19q codeletion using quantitative texture analysis [35], and *IDH*-mutant tumors may be less characterized by imaging features in the cohorts of lower-grade gliomas. Nonetheless, novel techniques, such as comprehensive machine-learning classification and detection of 2-hydroxyglutarate accumulated in *IDH*-mutated gliomas by proton MR spectroscopy hold substantial promise for clinical use in the future [3, 12, 22, 34].

Table 7 The relationship of the predictive score and 1p/19q codeletion in the validation cohort

1p/19q score	1p/19q codeleted	1p/19q non-codeleted	PPV (%)
Score 0	1	5	16.7 (1/6)
Score 1	3	14	17.6 (3/17)
Score 2	2	17	10.5 (2/19)
Score 3	5	1	83.3 (5/6)
Score 4	4	0	100 (4/4)

PPV positive predictive value

Limitation of the present study

Although our scoring systems by combination of some imaging features are likely to be less affected by inter-observer difference as compared with the evaluation of single imaging feature, the visual, qualitative analysis would still suffer from subjective nature. Moreover, judgment of each imaging feature could be affected by MRI parameters, field strength, and systems of imaging. Nonetheless, the preoperative assessment based on routine imaging information would be useful for therapeutic decision-making until novel quantitative techniques become widely accessible.

Most of the grade IV tumors are preoperatively distinguished from lower-grade gliomas typically by ring enhancement and extensive perifocal edema. However, the present cohorts did not include grade IV tumors, and it should be noted that those tumors with atypical images might not be distinguished from lower-grade gliomas by routine MRI.

Finally, our scoring system was established and validated using two independent cohorts; however, the sample size was relatively small. It is desirable to validate the scoring system in the larger cohort prospectively.

Table 8 The relationship of the predictive score and *MGMT* promoter methylation in the validation cohort

MGMT score	MGMT methylated	MGMT unmethylated	PPV (%)
Score 0	0	2	0 (0/2)
Score 1	11	9	55 (11/20)
Score 2	16	7	69.6 (16/23)
Score 3	6	1	85.7 (6/7)

MGMT O6-methylguanine-DNA methyltransferase, *PPV* positive predictive value

Conclusions

In conclusion, we established the scoring systems for preoperative diagnosis for 1p/19q codeletion and *MGMT* promoter methylation based on imaging features available on routine CT and MRI. The predictive values including sensitivity and specificity appear acceptable especially for 1p/19q codeletion, and these scoring systems would help to design overall treatment strategy and surgical strategy preoperatively.

Acknowledgements We greatly thank Ms. Naoko Tsuzaki at Department of Neurosurgery, Keio University School of Medicine for technical assistance of laboratory works. The authors also greatly thank Dr. Takayuki Abe at Center for Clinical Research, Department of Preventive Medicine and Public Health, Keio University School of Medicine, for statistical advice.

Compliance with ethical standards

Conflict of interest The authors declare that they have no conflict of interest.

Ethical approval This study has been conducted as a part of the collaborative translational research approved by the Institutional Review Board at Keio University and Fujita Health University. All procedures performed in studies involving human participants were in accordance with the ethical standards of the institutional and/or national research committee and with the 1964 Helsinki declaration and its later amendments or comparable ethical standards.

Informed consent Informed consent was obtained from all individual participants included in the study.

References

1. Brown R, Zlatescu M, Sijben A, Roldan G, Easaw J, Forsyth P, Parney I, Sevick R, Yan E, Demetrick D, Schiff D, Cairncross G, Mitchell R (2008) The use of magnetic resonance imaging to noninvasively detect genetic signatures in oligodendroglioma. Clin Cancer Res: Off J Am Assoc Cancer Res 14:2357–2362. https://doi.org/10.1158/1078-0432.ccr-07-1964
2. Cairncross JG, Ueki K, Zlatescu MC, Lisle DK, Finkelstein DM, Hammond RR, Silver JS, Stark PC, Macdonald DR, Ino Y, Ramsay DA, Louis DN (1998) Specific genetic predictors of chemotherapeutic response and survival in patients with anaplastic oligodendrogliomas. J Natl Cancer Inst 90:1473–1479
3. Choi C, Ganji SK, DeBerardinis RJ, Hatanpaa KJ, Rakheja D, Kovacs Z, Yang XL, Mashimo T, Raisanen JM, Marin-Valencia I, Pascual JM, Madden CJ, Mickey BE, Malloy CR, Bachoo RM, Maher EA (2012) 2-hydroxyglutarate detection by magnetic resonance spectroscopy in IDH-mutated patients with gliomas. Nat Med 18:624–629. https://doi.org/10.1038/nm.2682
4. Drabycz S, Roldan G, de Robles P, Adler D, McIntyre JB, Magliocco AM, Cairncross JG, Mitchell JR (2010) An analysis of image texture, tumor location, and MGMT promoter methylation in glioblastoma using magnetic resonance imaging. NeuroImage 49:1398–1405. https://doi.org/10.1016/j.neuroimage.2009.09.049
5. Ellingson BM, Cloughesy TF, Pope WB, Zaw TM, Phillips H, Lalezari S, Nghiemphu PL, Ibrahim H, Naeini KM, Harris RJ, Lai A (2012) Anatomic localization of O6-methylguanine DNA methyltransferase (MGMT) promoter methylated and unmethylated tumors: a radiographic study in 358 de novo human glioblastomas. NeuroImage 59:908–916. https://doi.org/10.1016/j.neuroimage.2011.09.076
6. Eoli M, Menghi F, Bruzzone MG, De Simone T, Valletta L, Pollo B, Bissola L, Silvani A, Bianchessi D, D'Incerti L, Filippini G, Broggi G, Boiardi A, Finocchiaro G (2007) Methylation of O6-methylguanine DNA methyltransferase and loss of heterozygosity on 19q and/or 17p are overlapping features of secondary glioblastomas with prolonged survival. Clin Cancer Res: Off J Am Assoc Cancer Res 13:2606–2613. https://doi.org/10.1158/1078-0432.CCR-06-2184
7. Ezaki T, Sasaki H, Hirose Y, Miwa T, Yoshida K, Kawase T (2011) Molecular characteristics of pediatric non-ependymal, nonpilocytic gliomas associated with resistance to temozolomide. Mol Med Rep 4:1101–1105. https://doi.org/10.3892/mmr.2011.573
8. Gupta A, Omuro AM, Shah AD, Graber JJ, Shi W, Zhang Z, Young RJ (2012) Continuing the search for MR imaging biomarkers for MGMT promoter methylation status: conventional and perfusion MRI revisited. Neuroradiology 54:641–643. https://doi.org/10.1007/s00234-011-0970-z
9. Hayashi S, Kitamura Y, Hirose Y, Yoshida K, Sasaki H (2017) Molecular-genetic and clinicopathological prognostic factors in patients with gliomas showing total 1p19q loss: gain of chromosome 19p and histological grade III negatively correlate with patient's prognosis. J Neuro-Oncol 132:119–126. https://doi.org/10.1007/s11060-016-2344-1
10. Hirose Y, Aldape K, Takahashi M, Berger MS, Feuerstein BG (2001) Tissue microdissection and degenerate oligonucleotide primed-polymerase chain reaction (DOP-PCR) is an effective method to analyze genetic aberrations in invasive tumors. J Mol Diagn: JMD 3:62–67. https://doi.org/10.1016/s1525-1578(10)60653-8
11. Jenkinson MD, Smith TS, Joyce KA, Fildes D, Broome J, du Plessis DG, Haylock B, Husband DJ, Warnke PC, Walker C (2006) Cerebral blood volume, genotype and chemosensitivity in oligodendroglial tumours. Neuroradiology 48:703–713. https://doi.org/10.1007/s00234-006-0122-z
12. Kalinina J, Carroll A, Wang L, Yu Q, Mancheno DE, Wu S, Liu F, Ahn J, He M, Mao H, Van Meir EG (2012) Detection of "oncometabolite" 2-hydroxyglutarate by magnetic resonance analysis as a biomarker of IDH1/2 mutations in glioma. J Mol Med 90:1161–1171. https://doi.org/10.1007/s00109-012-0888-x
13. Kleihues P, Burger PC, Scheithauer BW (1993) Histological typing of tumors of the central nervous system, 2nd edn. Springer, Berlin
14. Kleihues P, Cavanee W (2000) Pathology and genetics of tumors of the nervous system. International Agency for Research on Cancer Press, Lyon
15. Korfiatis P, Kline TL, Coufalova L, Lachance DH, Parney IF, Carter RE, Buckner JC, Erickson BJ (2016) MRI texture features as biomarkers to predict MGMT methylation status in glioblastomas. Med Phys 43:2835–2844. https://doi.org/10.1118/1.4948668
16. Louis DN, Ohgaki H, Wiestler OD, Cavenee WK (2007) WHO classification of tumours of the central nervous system, 4th edn. International agency for research on cancer, Lyon
17. Louis DN, Ohgaki H, Wiestler OD, Cavenee WK, Ellison DW, Figarella-Branger D, Perry A, Reifenberger G, von Deimling A (2016) WHO classification of tumours of the central nervous system. Revised 4th Edition edn. International agency for research on cancer, Lyon
18. Megyesi JF, Kachur E, Lee DH, Zlatescu MC, Betensky RA, Forsyth PA, Okada Y, Sasaki H, Mizoguchi M, Louis DN, Cairncross JG (2004) Imaging correlates of molecular signatures in oligodendrogliomas. Clin Cancer Res: Off J Am Assoc Cancer Res 10:4303–4306. https://doi.org/10.1158/1078-0432.ccr-04-0209

19. Miwa T, Hirose Y, Sasaki H, Ezaki T, Yoshida K, Kawase T (2011) Single-copy gain of chromosome 1q is a negative prognostic marker in pediatric nonependymal, nonpilocytic gliomas. Neurosurgery 68:206–212. https://doi.org/10.1227/NEU.0b013e3181fd2c2e
20. Miwa T, Hirose Y, Sasaki H, Ikeda E, Yoshida K, Kawase T (2009) Genetic characterization of adult infratentorial gliomas. J Neuro-Oncol 91:251–255. https://doi.org/10.1007/s11060-008-9714-2
21. Nishiyama Y, Sasaki H, Nagahisa S, Adachi K, Hayashi T, Yoshida K, Kawase T, Hattori N, Murayama K, Abe M, Hasegawa M, Hirose Y (2014) Radiological features of supratentorial gliomas are associated with their genetic aberrations. Neurosurg Rev 37: 291–299; discussion 299-300. https://doi.org/10.1007/s10143-013-0515-5
22. Pope WB, Qiao XJ, Kim HJ, Lai A, Nghiemphu P, Xue X, Ellingson BM, Schiff D, Aregawi D, Cha S, Puduvalli VK, Wu J, Yung WK, Young GS, Vredenburgh J, Barboriak D, Abrey LE, Mikkelsen T, Jain R, Paleologos NA, Rn PL, Prados M, Goldin J, Wen PY, Cloughesy T (2012) Apparent diffusion coefficient histogram analysis stratifies progression-free and overall survival in patients with recurrent GBM treated with bevacizumab: a multi-center study. J Neuro-Oncol 108:491–498. https://doi.org/10.1007/s11060-012-0847-y
23. Qi S, Yu L, Li H, Ou Y, Qiu X, Ding Y, Han H, Zhang X (2014) Isocitrate dehydrogenase mutation is associated with tumor location and magnetic resonance imaging characteristics in astrocytic neoplasms. Oncol Lett 7:1895–1902. https://doi.org/10.3892/ol.2014.2013
24. Saito T, Maruyama T, Muragaki Y, Tanaka M, Nitta M, Shinoda J, Aki T, Iseki H, Kurisu K, Okada Y (2013) 11C-methionine uptake correlates with combined 1p and 19q loss of heterozygosity in oligodendroglial tumors. AJNR Am J Neuroradiol 34:85–91. https://doi.org/10.3174/ajnr.A3173
25. Sanai N, Berger MS (2008) Glioma extent of resection and its impact on patient outcome. Neurosurgery 62:753–764 discussion 264-756
26. Sasaki H, Hirose Y, Yazaki T, Kitamura Y, Katayama M, Kimura T, Fujiwara H, Toda M, Ohira T, Yoshida K (2015) Upfront chemotherapy and subsequent resection for molecularly defined gliomas. J Neuro-Oncol 124:127–135. https://doi.org/10.1007/s11060-015-1817-y
27. Sasaki H, Zlatescu MC, Betensky RA, Ino Y, Cairncross JG, Louis DN (2001) PTEN is a target of chromosome 10q loss in anaplastic oligodendrogliomas and PTEN alterations are associated with poor prognosis. Am J Pathol 159:359–367. https://doi.org/10.1016/s0002-9440(10)61702-6
28. Smith JS, Chang EF, Lamborn KR, Chang SM, Prados MD, Cha S, Tihan T, Vandenberg S, McDermott MW, Berger MS (2008) Role of extent of resection in the long-term outcome of low-grade hemispheric gliomas. J Clin Oncol: Off J Am Soc Clin Oncol 26:1338–1345. https://doi.org/10.1200/JCO.2007.13.9337
29. Sonoda Y, Shibahara I, Kawaguchi T, Saito R, Kanamori M, Watanabe M, Suzuki H, Kumabe T, Tominaga T (2015) Association between molecular alterations and tumor location and MRI characteristics in anaplastic gliomas. Brain Tumor Pathol 32: 99–104. https://doi.org/10.1007/s10014-014-0211-3
30. van den Bent MJ, Baumert B, Erridge SC, Vogelbaum MA, Nowak AK, Sanson M, Brandes AA, Clement PM, Baurain JF, Mason WP, Wheeler H, Chinot OL, Gill S, Griffin M, Brachman DG, Taal W, Ruda R, Weller M, McBain C, Reijneveld J, Enting RH, Weber DC, Lesimple T, Clenton S, Gijtenbeek A, Pascoe S, Herrlinger U, Hau P, Dhermain F, van Heuvel I, Stupp R, Aldape K, Jenkins RB, Dubbink HJ, Dinjens WNM, Wesseling P, Nuyens S, Golfinopoulos V, Gorlia T, Wick W, Kros JM (2017) Interim results from the CATNON trial (EORTC study 26053-22054) of treatment with concurrent and adjuvant temozolomide for 1p/19q non-co-deleted anaplastic glioma: a phase 3, randomised, open-label intergroup study. Lancet (Lond, Engl) 390:1645–1653. https://doi.org/10.1016/s0140-6736(17)31442-3
31. Walker C, du Plessis DG, Fildes D, Haylock B, Husband D, Jenkinson MD, Joyce KA, Broome J, Kopitski K, Prosser J, Smith T, Vinjamuri S, Warnke PC (2004) Correlation of molecular genetics with molecular and morphological imaging in gliomas with an oligodendroglial component. Clin Cancer Res: Off J Am Assoc Cancer Res 10:7182–7191. https://doi.org/10.1158/1078-0432.CCR-04-0681
32. Xiong J, Tan W, Wen J, Pan J, Wang Y, Zhang J, Geng D (2016) Combination of diffusion tensor imaging and conventional MRI correlates with isocitrate dehydrogenase 1/2 mutations but not 1p/19q genotyping in oligodendroglial tumours. Eur Radiol 26:1705–1715. https://doi.org/10.1007/s00330-015-4025-4
33. Yan H, Parsons DW, Jin G, McLendon R, Rasheed BA, Yuan W, Kos I, Batinic-Haberle I, Jones S, Riggins GJ, Friedman H, Friedman A, Reardon D, Herndon J, Kinzler KW, Velculescu VE, Vogelstein B, Bigner DD (2009) IDH1 and IDH2 mutations in gliomas. N Engl J Med 360:765–773. https://doi.org/10.1056/NEJMoa0808710
34. Zhang B, Chang K, Ramkissoon S, Tanguturi S, Bi WL, Reardon DA, Ligon KL, Alexander BM, Wen PY, Huang RY (2017) Multimodal MRI features predict isocitrate dehydrogenase genotype in high-grade gliomas. Neuro-Oncology 19:109–117. https://doi.org/10.1093/neuonc/now121
35. Zhou H, Vallieres M, Bai HX, Su C, Tang H, Oldridge D, Zhang Z, Xiao B, Liao W, Tao Y, Zhou J, Zhang P, Yang L (2017) MRI features predict survival and molecular markers in diffuse lower-grade gliomas. Neuro-Oncology 19:862–870. https://doi.org/10.1093/neuonc/now256
36. Zlatescu MC, TehraniYazdi A, Sasaki H, Megyesi JF, Betensky RA, Louis DN, Cairncross JG (2001) Tumor location and growth pattern correlate with genetic signature in oligodendroglial neoplasms. Cancer Res 61:6713–6715
37. Zulch KJ (1979) Histological typing of tumors of the central nervous system. World Health Organization, Genova